2 Constrained Density-Functional Theory: Formalism, Algorithms and Applications

Xavier Gonze
IMCN, Université catholique de Louvain
8, chemin de l'observatoire, B-1348 Louvain-la-neuve

Contents

1 Introduction **2**

2 Background: density-functional theory **4**
2.1 Hohenberg-Kohn and Kohn-Sham theorems 4
2.2 Spin-dependent generalization of the basic theorems 7
2.3 Approximate exchange-correlation functionals 10
2.4 Algorithms for the self consistency 11

3 Constrained density-functional theory: formalism and approximations **13**
3.1 Formal constrained density-functional theory 14
3.2 Constraints at the Hohenberg-Kohn level 15
3.3 Constrained density-functional theory at the Kohn-Sham level 17

4 Constrained density-functional theory algorithms **18**
4.1 Microiterations 18
4.2 Penalty function approaches 19
4.3 Lagrange multipliers again: a potential-based SCF approach 20

5 Some applications of constrained density-functional theory **22**

6 Conclusion **28**

E. Pavarini and E. Koch (eds.)
Correlated Materials: Methods and Applications
Modeling and Simulation Vol. 16, Forschungszentrum Jülich, 2026
ISBN 978-3-95806-909-1 http://www.cond-mat.de/events/correl26

1 Introduction

The vast majority of first-principles simulations of ground-state properties of molecules, condensed matter and nanosystems relies on density-functional theory (DFT) [1, 2]. Over the last decades, DFT has achieved remarkable success, providing a broadly applicable and computationally efficient framework to describe the structural, electronic, magnetic, and vibrational properties of a wide variety of systems. It has enabled predictive simulations of complex materials, accurate total energies, forces and response functions, and has become the workhorse of modern materials science and quantum chemistry [3].

Despite these achievements, DFT also exhibits well-known limitations [4, 5]. These limitations become particularly severe in systems where electron-electron interactions play a dominant role, such as transition-metal oxides, heavy fermion compounds, or strongly correlated molecular systems. In these cases, standard approximations to the exchange-correlation functional may fail to capture key physical phenomena, including Mott insulating behavior, charge localization, or dynamical spectral properties [5]. More generally, the static and mean-field nature of conventional DFT functionals makes them ill-suited for describing strong correlation effects and the associated many-body excitations.

To overcome these difficulties, more advanced theoretical frameworks have been developed. Among them, dynamical mean-field theory (DMFT) is a powerful approach to treat local electronic correlations beyond the mean-field level, by mapping the lattice problem onto an effective quantum impurity model embedded in a self-consistently determined bath. [6, 5]. The combination of DFT and DMFT (DFT+DMFT) has proven particularly successful, allowing one to retain the realistic band-structure description provided by DFT while capturing the dynamical correlations characteristic of strongly correlated materials. One extracts from DFT localized orbitals, determines hopping parameters, and estimates interaction strengths (the Hubbard-U) entering DMFT calculations [7]. For example, the parameters of the Hubbard model, here written for the single-band case, can all be determined

$$\hat{H} = -\sum_{\langle ij\rangle,\sigma} t_{ij}\, \hat{c}^{\dagger}_{i\sigma}\hat{c}_{j\sigma} + U \sum_{i} \hat{n}_{i\uparrow}\hat{n}_{i\downarrow}, \tag{1}$$

where i, j label lattice sites, $\langle i, j\rangle$ denotes pairs of sites coupled by hopping, $\sigma = \uparrow, \downarrow$ is the spin index, $\hat{c}^{\dagger}_{i\sigma}$ and $\hat{c}_{i\sigma}$ are fermionic creation and annihilation operators, t_{ij} is the hopping amplitude between sites i and j, $\hat{n}_{i\sigma}$ is the number operator at site i for spin σ, and U is the on-site Coulomb interaction.

In the general context of the simulation of real materials based on model many-body Hamiltonians, DFT plays an essential, albeit auxiliary role, as it provides the underlying one-electron Hamiltonian and effective interactions and enables the construction of low-energy effective models. It also allows one to identify relevant degrees of freedom and to construct corresponding many-body models.

Even if not explicitly mentioned, such usage of DFT beyond electronic ground state calculations is often based on constrained density-functional theory (cDFT), introduced in 1984 by

Dederichs and coworkers [8]. cDFT provides a versatile framework to access states and observables beyond the ground state, and to define physically meaningful quantities such as local charges, magnetizations, or interaction parameters [4].

Beyond finding the parameters for DMFT calculations, cDFT is routinely applied in several other fields of research. Constraining the charge on some molecular fragments allows one to explore the gradual transfer of an electron from one fragment to another, and provide parameters for Marcus theory [9, 10]. Constraining the spin magnetization in the neighborhood of an atom inside a solid allows one to obtain the energy of the system as a function of the local magnetization [8].

In this respect, and as a second example of a model Hamiltonian amenable to definition from cDFT, all the parameters of a Heisenberg model including isotropic exchange (J_{ij}), Dzyaloshinskii-Moriya interaction $(\mathbf{D}_{ij})$, and single-ion anisotropy (A_i), for a set of atoms labelled with i and j, with local spin magnetization vectors $\mathbf{S}_i$ and $\mathbf{S}_j$ [11–14]

$$H = -\sum_{\langle ij \rangle} J_{ij}\, \mathbf{S}_i \cdot \mathbf{S}_j - \sum_{\langle ij \rangle} \mathbf{D}_{ij} \cdot (\mathbf{S}_i \times \mathbf{S}_j) - \sum_i A_i (S_i^z)^2, \tag{2}$$

can, in principle, be extracted using constrained DFT for a given real magnetic material.

The specification of local magnetization or local charge can be combined with more usual variables governing the energy in first-principle calculations, like the atomic positions or cell parameters. Thus cDFT can provide parameters for models of magnetic state of matter (including Heisenberg model), with the associated description of magnons [8, 15, 16], but also their coupling of phonons. Similarly, parameters can be obtained for second-principles models [17–20], or for constituting training sets for the fitting of machine-learning interatomic potentials [21–24].

The implementations and applications of cDFT over the years have been numerous, and, for chemistry, have been reviewed by Kaduk and Van Voorhis in 2012 [4]. In 2016, a list of existing implementations has been collected by Melander and coworkers [25]. Then, one further implementation has been described by Hegde and coworkers [26]. The field being enormous, it will not be the purpose of the present lecture to cover all implementations or applications of cDFT, but to provide relevant entry points in the literature, and provide some examples of applications.

Several methods have been proposed to impose the constraints. In the first one [27, 4], an inner "micro"-self-consistency loop is added to the usual DFT self-consistency loop. In this inner loop, the potential (or local magnetic field) is varied to impose the constraint. In another one [28, 29], a penalty function is added to the energy functional. Recently, a potential-based self-consistency approach capable of placing the local magnetization, fragment charge, atomic positions and stresses on a par has been proposed and applied [30].

The present lecture is organized as follows. In Sec. 2, I recall the fundamental aspects of density-functional theory, including its spin-dependent generalization, approximations to the exchange-correlation functional, and the algorithms used to achieve self-consistency. This background is essential to understand both the formal and practical extensions introduced by

constrained approaches. This section might obviously be skipped by those who have already a good command of DFT.
In Sec. 3, the formal framework of constrained density-functional theory is presented, emphasizing its foundation within the Hohenberg-Kohn variational principle and the Levy constrained-search formulation. The types of constraints that can be rigorously formulated at the many-body level are discussed, as well as those defined at the Kohn-Sham level. Then, the approximations that arise in practical implementations are mentioned.
In Sec. 4, I review the main algorithmic strategies used to enforce constraints in practice, including Lagrange-multiplier formulations, penalty-function approaches, and recent developments based on potential-based self-consistent schemes. Their respective advantages, limitations, and interconnections, are highlighted, while recent progress in unifying these approaches are mentioned.
Finally, in Sec. 5, some capabilities of constrained DFT are shown through representative applications. These include the determination of model Hamiltonian parameters such as the Hubbard U, the exploration of magnetic energy landscapes and magnetoelastic coupling, and recent advances in dynamical response theory. In particular, I show how constrained density-functional perturbation theory provides access to nonadiabatic spin dynamics and reveals novel physical effects such as the emergence of a finite magnon mass.
The paper concludes in Sec. 6 with a summary of the main concepts and an outlook on future developments and applications of constrained DFT.
Atomic units ($|e| = 1$, m_e=1, $\hbar = 1$) are used throughout.

2 Background: density-functional theory

Density-functional theory (DFT) provides a formally exact framework to determine the ground-state properties of interacting electrons in an external potential v_{ext}. Its practical implementation relies on an effective single-particle description and on iterative self-consistency algorithms. In this section, I recall the main concepts that will be used in the later sections, including its spin generalizations, both collinear and non-collinear. Many readers, already knowledgeable of DFT, might skip this section, to dive directly in constrained density-functional theory specificities.

2.1 Hohenberg-Kohn and Kohn-Sham theorems

Hohenberg-Kohn theorems. The theoretical foundation of DFT is provided by the Hohenberg–Kohn (HK) theorems [31]. For a system of N interacting electrons in a local external one-body potential $v_{\text{ext}}(\mathbf{r})$, where the interaction $\hat{V}_{ee}$ is considered fixed while the external potential is allowed to vary, the first theorem establishes a one-to-one correspondence between the ground-state density $\rho(\mathbf{r})$ and the external potential (up to an additive constant). As a consequence, the ground-state density determines the Hamiltonian,

$$\hat{H}[\rho] = \hat{T} + \hat{V}_{ee} + \hat{v}_{\text{ext}}[\rho], \tag{3}$$

where $\hat{T}$ is the kinetic energy operator, and all properties (not only ground-state ones) are (formally) unique functionals of the ground-state density, except for the possible dependence on the above-mentioned additive constant.

The second HK theorem introduces a variational principle: for a given interaction $\hat{V}_{ee}$, there exists an universal functional $F[\rho]$, independent of v_{ext}, such that the ground-state energy is obtained by minimizing

$$E_{v_{\text{ext}}}[\rho] = F[\rho] + \int \rho(\mathbf{r}) v_{\text{ext}}(\mathbf{r})\, d\mathbf{r}. \tag{4}$$

The exact ground-state energy is thus

$$E^{\text{GS}}_{v_{\text{ext}}} = \min_{\rho \to N} E_{v_{\text{ext}}}[\rho], \tag{5}$$

where $\rho \to N$ indicates that the electronic density integrates to N in the whole space.

The functional $F[\rho]$ is formally defined as

$$F[\rho] = \big\langle \Psi[\rho] \big| \, \hat{T} + \hat{V}_{ee} \, \big| \Psi[\rho] \big\rangle, \tag{6}$$

where $\Psi[\rho]$ is the interacting many-electron ground-state wavefunction obtained from the first HK theorem. This approach has the caveat that the set of densities over which the minimization has to be performed only includes those that are v-representable, that is, those that correspond to the ground state of a Hamiltonian for the defined interaction $\hat{V}_{ee}$ with some external local potential.

Levy constrained search approach. A rigorous formulation avoiding the notion of v-representability has been provided by Levy [32]. In his constrained-search approach, the functional $F[\rho]$ is determined from

$$F[\rho] = \min_{\Psi \to \rho} \langle \Psi | \hat{T} + \hat{V}_{ee} | \Psi \rangle, \tag{7}$$

the minimization being performed over all antisymmetric wavefunctions yielding the density ρ. This formulation is particularly useful conceptually, as it emphasizes that DFT is fundamentally a variational theory over densities. $F[\rho]$ contains all the many-body effects (kinetic + interaction). However, its explicit form is unknown. This expression serves primarily as an existence proof.

By the same token, the demonstration of the second HK theorem now becomes transparent. Indeed, the well-known extremal principle of quantum mechanics delivers

$$E_{v_{\text{ext}}} = \min_{\Psi \to N} \big\langle \Psi \big| \hat{H}_{v_{\text{ext}}} \big| \Psi \big\rangle. \tag{8}$$

In order to prove the second HK theorem, an intermediate minimization over charge densities is introduced,

$$E_{v_{\text{ext}}} = \min_{\rho \to N} \Big\{ \min_{\Psi \to \rho} \big\langle \Psi \big| \hat{H}_{v_{\text{ext}}} \big| \Psi \big\rangle \Big\}, \tag{9}$$

as above, the Hamiltonian is decomposed,

$$\hat{H}_{v_{\text{ext}}} = \hat{T} + \hat{V}_{ee} + \hat{v}_{\text{ext}}, \tag{10}$$

so that, using the one-body characteristic of the external potential operator, one obtains:

$$E_{v_{\rm ext}} = \min_{\rho \to N} \left\{ \min_{\Psi \to \rho} \left[\left\langle \Psi \middle| \hat{T} + \hat{V}_{ee} \middle| \Psi \right\rangle + \int \rho(\mathbf{r})\, v_{\rm ext}(\mathbf{r})\, d\mathbf{r} \right] \right\}. \tag{11}$$

With the definition of the universal functional $F[\rho]$, Eq. (7) the variational problem becomes:

$$E_{v_{\rm ext}} = \min_{\rho \to N} \left\{ F[\rho] + \int \rho(\mathbf{r})\, v_{\rm ext}(\mathbf{r})\, d\mathbf{r} \right\} = \min_{\rho \to N} E_{v_{\rm ext}}[\rho]. \tag{12}$$

With such a relation, in mathematical terms, $E_{v_{\rm ext}}$ and $F[\rho]$ are related to each other by a Legendre transform.

Kohn-Sham mapping to non-interacting fermions. The Kohn-Sham (KS) approach [33] provides a practical scheme to evaluate the ground-state density by mapping the interacting many-electron system onto an auxiliary system of non-interacting fermions reproducing the same density.

Kohn and Sham observed that the Hohenberg-Kohn theorems can be applied to interacting electrons, but also to non-interacting electrons. In the latter case, the ground-state of the many-body problem is known: a set of one-particle wavefunctions forming a Slater determinant (non-interacting electrons) to fulfill the antisymmetry requirement. They subtracted from the $F[\rho]$ functional the non-interacting electron kinetic energy $T_{\rm s}[\rho]$ and the classical electrostatic energy of the electronic density (the so-called Hartree energy), $E_{\rm H}[\rho]$, to define the exchange-correlation (xc) energy functional, incorporating all many-body effects beyond the classical electrostatic interaction

$$E_{\rm xc}[\rho] = F[\rho] - T_{\rm s}[\rho] - E_{\rm H}[\rho], \tag{13}$$

with

$$T_{\rm s}[\rho] = \min_{\Psi \to \rho} \langle \Psi | \hat{T} | \Psi \rangle, \tag{14}$$

and

$$E_{\rm H}[\rho] = \frac{1}{2} \int \frac{\rho(\mathbf{r})\, \rho(\mathbf{r}')}{|\mathbf{r} - \mathbf{r}'|}\, d\mathbf{r}\, d\mathbf{r}'. \tag{15}$$

Matching the variational principles for the interacting and non-interacting electron cases, they derived a variational principle for the energy of a set of N "fictitious" non-interacting electrons as a functional of orthonormal one-electron occupied wavefunctions $\{\phi_i\}$

$$E^{\phi_i}_{v_{\rm ext}}[\{\phi_i\}] = T_{\rm s}[\{\phi_i\}] + \int \rho[\{\phi_i\}](\mathbf{r})\, v_{\rm ext}(\mathbf{r})\, d\mathbf{r} + E_{\rm Hxc}[\rho[\{\phi_i\}]], \tag{16}$$

with non-interacting kinetic energy and electronic density given now in terms of the non-interacting independent wavefunctions by

$$T_{\rm s}[\{\phi_i\}] = \sum_i f_i \langle \phi_i | \hat{T} | \phi_i \rangle, \tag{17}$$

and

$$\rho[\{\phi_i\}](\mathbf{r}) = \sum_i f_i \phi_i^*(\mathbf{r}) \phi_i(\mathbf{r}), \tag{18}$$

f_i being occupation numbers (e.g., $f_i = 2$ for doubly occupied wavefunctions, spin up and spin down, 0 otherwise).
The stationary condition of the functional $E^{\phi_i}_{v_{\text{ext}}}[\{\phi_i\}]$ under orthonormality constraints leads to the following set of equations (an unitary transformation is performed to obtain eigenfunctions)

$$\big(\hat{T} + \hat{v}\big)|\phi_i\rangle = \varepsilon_i|\phi_i\rangle, \tag{19}$$

with the "Kohn-Sham" potential (the external potential screened by the potential created by the non-interacting electrons) defined as

$$v[\rho](\mathbf{r}) = v_{\text{ext}}(\mathbf{r}) + v_{\text{Hxc}}[\rho](\mathbf{r}), \tag{20}$$

with

$$v_{\text{Hxc}}[\rho](\mathbf{r}) = \frac{\delta E_{\text{Hxc}}}{\delta\rho(\mathbf{r})}, \tag{21}$$

or equivalently,

$$v_{\text{Hxc}}[\rho](\mathbf{r}) = \int \frac{\rho(\mathbf{r}')}{|\mathbf{r}-\mathbf{r}'|}\, d\mathbf{r}' + \frac{\delta E_{\text{xc}}}{\delta\rho(\mathbf{r})}, \tag{22}$$

and the density being obtained from the wavefunctions following Eq. (18).
The Kohn-Sham equations must be solved self-consistently, since the potential depends on the density, itself constructed from the one-electron wavefunctions. This will be examined further in Sec. 2.4.

2.2 Spin-dependent generalization of the basic theorems

The Hohenberg-Kohn and Kohn-Sham frameworks can be generalized to systems with spin degrees of freedom, as established by von Barth and Hedin [34]. In the general (non-collinear) case, the electronic state is described by a spinorial wavefunction $|\Psi\rangle$ (each electron spatial argument is complemented with a spinor argument), and the basic variable is the spin-density matrix $\rho_{\alpha\beta}(\mathbf{r})$. The values of α and β can be $\uparrow$ or $\downarrow$. The spin-density matrix can be decomposed as

$$\rho_{\alpha\beta}(\mathbf{r}) = \frac{1}{2}\rho(\mathbf{r})\,\delta_{\alpha\beta} + \frac{1}{2}\mathbf{m}(\mathbf{r})\cdot\boldsymbol{\sigma}_{\alpha\beta}, \tag{23}$$

where $\mathbf{m}(\mathbf{r})$ is the local magnetization density, $\rho(\mathbf{r})$ is the scalar electronic density (the trace of the density matrix), and $\boldsymbol{\sigma}$ is the vector of Pauli matrices. The external potential becomes spin dependent and can be represented as a Hermitian matrix $v_{\text{ext},\alpha\beta}(\mathbf{r})$, which may equivalently be decomposed into a scalar potential and a magnetic field. In the collinear case, the spin-density matrix reduces to the pair of diagonal spin densities $\rho^{\uparrow}(\mathbf{r})$ and $\rho^{\downarrow}(\mathbf{r})$, and similarly for the external potential.

Spin-dependent Hohenberg-Kohn theorem. In the spin-dependent case, a naive extension of the first Hohenberg-Kohn theorem is not sufficient, since spin-dependent potentials with different longitudinal magnetic field may yield the same spin density (see the Appendix of Ref. [34]), referred to as the magnetic field gauge freedom. However, it can still be shown that,

for a non-degenerate ground state, the many-body wavefunction is uniquely determined by the spin-density matrix $\rho_{\alpha\beta}(\mathbf{r})$, and therefore all ground-state properties that do not depend on the magnetic field gauge are functionals of this quantity.
The corresponding variational principle generalizes straightforwardly

$$E_{v_{\text{ext}}}[\rho_{\alpha\beta}] = F[\rho_{\alpha\beta}] + \int \rho_{\alpha\beta}(\mathbf{r})\, v_{\text{ext},\beta\alpha}(\mathbf{r})\, d\mathbf{r}, \tag{24}$$

with

$$E^{\text{GS}}_{v_{\text{ext}}} = \min_{\rho_{\alpha\beta}\to N} E_{v_{\text{ext}}}[\rho_{\alpha\beta}], \tag{25}$$

and the universal functional F defined through the constrained search is

$$F[\rho_{\alpha\beta}] = \min_{\Psi\to\rho_{\alpha\beta}} \big\langle \Psi \big| \hat{T} + \hat{V}_{ee} \big| \Psi \big\rangle. \tag{26}$$

Spin-dependent Kohn-Sham equations (non-collinear case). Following the same strategy as in the spin-independent case, one introduces a non-interacting system reproducing the spin-density matrix. The exchange-correlation functional is formally introduced as

$$E_{\text{xc}}[\rho_{\alpha\beta}] = F[\rho_{\alpha\beta}] - T_{\text{s}}[\rho_{\alpha\beta}] - E_{\text{H}}[\rho]. \tag{27}$$

The energy functional is then written as

$$E_{v_{\text{ext}}}[\rho_{\alpha\beta}] = T_{\text{s}}[\rho_{\alpha\beta}] + \int \rho_{\alpha\beta}(\mathbf{r})\, v_{\text{ext},\beta\alpha}(\mathbf{r})\, d\mathbf{r} + E_{\text{H}}[\rho] + E_{\text{xc}}[\rho_{\alpha\beta}], \tag{28}$$

where $\rho(\mathbf{r}) = \sum_\alpha \rho_{\alpha\alpha}(\mathbf{r})$ is the scalar electronic density.
The non-interacting kinetic energy is expressed in terms of one-electron spinorial wavefunctions $|\Phi_i\rangle$, with spinor components $|\phi_{i\alpha}\rangle$,

$$T_{\text{s}}[\{\Phi_i\}] = \sum_{i\alpha} f_i \langle \phi_{i\alpha} | \hat{T} | \phi_{i\alpha} \rangle, \tag{29}$$

and the spin-density matrix is obtained from the occupied wavefunctions as

$$\rho_{\alpha\beta}(\mathbf{r}) = \sum_i f_i\, \phi^*_{i\alpha}(\mathbf{r}) \phi_{i\beta}(\mathbf{r}). \tag{30}$$

Occupation numbers f_i are $f_i = 1$ for occupied wavefunctions, 0 otherwise.
Minimization of the functional under orthonormality constraints leads to a set of coupled one-particle equations

$$\big(\hat{T} + \hat{v}\big) |\Phi_i\rangle = \varepsilon_i |\Phi_i\rangle, \tag{31}$$

where the effective potential is now a 2×2 Hermitian operator in spin space,

$$v_{\alpha\beta}(\mathbf{r}) = v_{\text{ext},\alpha\beta}(\mathbf{r}) + v_{\text{H}}(\mathbf{r})\, \delta_{\alpha\beta} + v_{\text{xc},\alpha\beta}(\mathbf{r}), \tag{32}$$

with the Hartree potential depending only on the scalar electronic density,

$$v_{\text{H}}(\mathbf{r}) = \int \frac{\rho(\mathbf{r}')}{|\mathbf{r}-\mathbf{r}'|}\, d\mathbf{r}', \tag{33}$$

and the exchange-correlation potential defined as the functional derivative

$$v_{\mathrm{xc},\alpha\beta}(\mathbf{r}) = \frac{\delta E_{\mathrm{xc}}[\rho_{\alpha\beta}]}{\delta \rho_{\beta\alpha}(\mathbf{r})}. \tag{34}$$

The Kohn-Sham equations thus take the form of matrix Schrödinger equations in spin space, and must be solved self-consistently since the potential depends on the spin-density matrix constructed from the spinor wavefunctions.

Similarly to the representation of the spin-density matrix, the effective potential can be written alternatively as

$$v_{\alpha\beta}(\mathbf{r}) = v_{\mathrm{ext},\alpha\beta}(\mathbf{r}) \; + v_{\mathrm{Hsxc}}(\mathbf{r})\, \delta_{\alpha\beta} + \frac{1}{2}\big(\mathbf{B}_{\mathrm{xc}}(\mathbf{r}) \cdot \boldsymbol{\sigma}\big)_{\alpha\beta}, \tag{35}$$

where v_{Hsxc} is a scalar potential (the Hartree potential plus half the trace of the xc potential) and $\mathbf{B}_{\mathrm{xc}}$ acts as an effective magnetic field.

In the spin collinear case, spin-flip components (off-diagonal) of the Hamiltonian vanish, the two spin channels separate, and the eigenfunctions are pure spin states (either up or down). Accordingly, the spin-density matrix is diagonal, there is no dependence of the exchange-correlation energy functional on the off-diagonal components of the density matrix, which cause (self-consistently) the spin-flip components of the Hamiltonian to vanish. Explicitly, the Kohn-Sham equations become spin dependent

$$\big(\hat{T} + \hat{v}_\sigma\big)|\phi_{i\sigma}\rangle = \varepsilon_{i\sigma}|\phi_{i\sigma}\rangle, \tag{36}$$

with $\sigma = \uparrow, \downarrow$, and effective potentials

$$v_\sigma(\mathbf{r}) = v_{\mathrm{ext}}(\mathbf{r}) + v_{\mathrm{H}}(\mathbf{r}) + v_{\mathrm{xc},\sigma}(\mathbf{r}), \tag{37}$$

where

$$v_{\mathrm{xc},\sigma}(\mathbf{r}) = \frac{\delta E_{\mathrm{xc}}[\rho^\uparrow, \rho^\downarrow]}{\delta \rho^\sigma(\mathbf{r})}. \tag{38}$$

The spin densities are obtained from the spin-resolved KS wavefunctions as

$$\rho^\sigma(\mathbf{r}) = \sum_i f_{i\sigma} \big|\phi_{i\sigma}(\mathbf{r})\big|^2. \tag{39}$$

The scalar charge density used in the Hartree potential is

$$\rho(\mathbf{r}) = \rho^\uparrow(\mathbf{r}) + \rho^\downarrow(\mathbf{r}). \tag{40}$$

While the collinear case covers ferromagnetic and antiferromagnetic materials, the non-collinear case leads to a fully coupled problem in spin space, which is essential for describing spin textures, spin spirals, spin-orbit coupling, and systems subject to spatially varying magnetic fields. In both collinear and non-collinear cases, the role of the exchange-correlation functional becomes more important than in the non-magnetic case, as the Hartree contribution does not encode any spin polarization effect, while such information is essential for the description of magnetic materials.

2.3 Approximate exchange-correlation functionals

In practice, the exact functional $E_{\rm xc}[\rho]$ is unknown and must be approximated. The simplest and historically most important approximation is the local density approximation (LDA) [33], in which

$$E_{\rm xc}^{\rm LDA}[\rho] = \int \rho(\mathbf{r})\, \varepsilon_{\rm xc}(\rho(\mathbf{r}))\, d\mathbf{r}, \tag{41}$$

where $\varepsilon_{\rm xc}$ is the exchange-correlation energy density of the homogeneous electron gas.
The LDA can be generalized to spin-polarized systems, leading to the local spin-density approximation (LSDA) [34]. The key idea is to use, at each point in space, the exchange-correlation energy density of a homogeneous electron gas with the same local spin polarization.

Collinear case. In the collinear case, the basic variables are the spin densities $\rho^{\uparrow}(\mathbf{r})$ and $\rho^{\downarrow}(\mathbf{r})$, or equivalently the total density $\rho(\mathbf{r})$ and the magnetization density $m(\mathbf{r}) = \rho^{\uparrow}(\mathbf{r}) - \rho^{\downarrow}(\mathbf{r})$. The LSDA functional is written as

$$E_{\rm xc}^{\rm LSDA}[\rho^{\uparrow}, \rho^{\downarrow}] = \int \rho(\mathbf{r})\, \varepsilon_{\rm xc}\big(\rho(\mathbf{r}), \zeta(\mathbf{r})\big)\, d\mathbf{r}, \tag{42}$$

where

$$\rho(\mathbf{r}) = \rho^{\uparrow}(\mathbf{r}) + \rho^{\downarrow}(\mathbf{r}), \qquad \zeta(\mathbf{r}) = \frac{\rho^{\uparrow}(\mathbf{r}) - \rho^{\downarrow}(\mathbf{r})}{\rho(\mathbf{r})} = \frac{m(\mathbf{r})}{\rho(\mathbf{r})}, \tag{43}$$

is the local spin polarization, and $\varepsilon_{\rm xc}(\rho, \zeta)$ is the exchange-correlation energy per particle of a homogeneous spin-polarized electron gas.
The corresponding exchange-correlation potentials are obtained as functional derivatives with respect to the spin densities,

$$v_{{\rm xc},\sigma}(\mathbf{r}) = \frac{\delta E_{\rm xc}^{\rm LSDA}}{\delta \rho^{\sigma}(\mathbf{r})}, \qquad \sigma = \uparrow, \downarrow, \tag{44}$$

which, using the chain rule, can be expressed in terms of derivatives of $\varepsilon_{\rm xc}(\rho, \zeta)$ with respect to ρ and ζ.

Non-collinear case. In the general non-collinear case, the exchange-correlation functional depends on the spin-density matrix $\rho_{\alpha\beta}(\mathbf{r})$, or equivalently on the pair $(\rho(\mathbf{r}), \mathbf{m}(\mathbf{r}))$. The LSDA is constructed by assuming that, locally, the system behaves as a homogeneous electron gas with density $\rho(\mathbf{r})$ and magnetization magnitude $|\mathbf{m}(\mathbf{r})|$. One thus defines

$$E_{\rm xc}^{\rm LSDA}[\rho_{\alpha\beta}] = \int \rho(\mathbf{r})\, \varepsilon_{\rm xc}\big(\rho(\mathbf{r}), \zeta(\mathbf{r})\big)\, d\mathbf{r}, \tag{45}$$

with

$$\zeta(\mathbf{r}) = \frac{|\mathbf{m}(\mathbf{r})|}{\rho(\mathbf{r})}, \tag{46}$$

so that the functional depends only on rotationally invariant quantities in spin space. In particular, it is invariant under global spin rotations, as required for a proper non-collinear formulation.

The exchange-correlation potential is then obtained as a functional derivative with respect to the spin-density matrix,

$$v_{\mathrm{xc},\alpha\beta}(\mathbf{r}) = \frac{\delta E_{\mathrm{xc}}^{\mathrm{LSDA}}}{\delta \rho_{\beta\alpha}(\mathbf{r})}\,. \tag{47}$$

Using the decomposition in scalar and vector components, it can be written as

$$v_{\mathrm{xc},\alpha\beta}(\mathbf{r}) = v_{\mathrm{sxc}}(\mathbf{r})\,\delta_{\alpha\beta} + \big(\mathbf{B}_{\mathrm{xc}}(\mathbf{r})\cdot\boldsymbol{\sigma}\big)_{\alpha\beta}, \tag{48}$$

where

$$v_{\mathrm{sxc}}(\mathbf{r}) = \frac{\partial(\rho\varepsilon_{\mathrm{xc}})}{\partial\rho}, \qquad \mathbf{B}_{\mathrm{xc}}(\mathbf{r}) = \frac{\partial(\rho\varepsilon_{\mathrm{xc}})}{\partial\mathbf{m}} = \frac{\partial(\rho\varepsilon_{\mathrm{xc}})}{\partial|\mathbf{m}|}\frac{\mathbf{m}(\mathbf{r})}{|\mathbf{m}(\mathbf{r})|}\,. \tag{49}$$

Within LSDA, the effective exchange-correlation magnetic field $\mathbf{B}_{\mathrm{xc}}(\mathbf{r})$ is therefore locally parallel to the magnetization density $\mathbf{m}(\mathbf{r})$. This property reflects the fact that the approximation is based on a homogeneous reference system without spatial spin texture.

Generalized gradient approximations (GGA), such as PBE [35], improve upon LDA by including gradient corrections

$$E_{\mathrm{xc}}^{\mathrm{GGA}}[\rho] = \int f\big(\rho(\mathbf{r}), \nabla\rho(\mathbf{r})\big)\,d\mathbf{r}. \tag{50}$$

GGAs can be generalized to the spin-dependent case, both collinear and non-collinear. More elaborate approximations include meta-GGAs and hybrid functionals [36], which incorporate additional non-local information or exact exchange contributions, with also spin-dependent generalizations.

Despite their successes, approximate functionals exhibit well-known limitations, including self-interaction errors and difficulties with strongly correlated systems. These limitations motivate extensions of DFT such as DFT+U [37, 1, 5] or constrained DFT, discussed in this lecture.

2.4 Algorithms for the self consistency

In this section, the discussion of self consistency applies generically to the non-spin-polarized, collinear spin-polarized and non-collinear spin-polarized cases. For sake of simplicity I have used the notation corresponding to the non-spin-polarized case. The adaptation to the other spin cases is rather easy.

The Kohn-Sham equations, Eqs. (18)–(22) define a non-linear self-consistent problem that is typically solved iteratively.

Eq. (20) delivers the effective Kohn-Sham potential (often denoted "screened" potential in the context of self-consistency) as a functional of the density. Similarly, one finds the density as a functional of the screened potential as follows. For a given trial screened potential u, associated with the local operator $\hat{u}$, one solves the corresponding Schrödinger equation

$$\big(\hat{T} + \hat{u}\big)|\phi_{i,u}\rangle = \varepsilon_{i,u}|\phi_{i,u}\rangle, \tag{51}$$

which yields a set of Kohn-Sham wavefunctions $|\phi_{i,u}\rangle$. These wavefunctions are then used in Eq. (18) to construct the electronic density, thereby defining the density as a functional of the potential, denoted ρ^{v}

$$\rho^{\mathrm{v}}[u] \triangleq \rho[\phi_{i,u}]. \tag{52}$$

The self-consistent density ρ^* is thus obtained as the fixed point of this mapping, satisfying

$$\rho^* = \rho^{\rm v}[v[\rho^*]]. \tag{53}$$

In these expressions, the density, the potential, and the wavefunctions all depend on the spatial coordinate. For conciseness, this explicit dependence, e.g., as in Eq. (18), is omitted here and in most of the following expressions.

Many iterative techniques [38–41] have been developed over the years to tackle the self-consistency problem, Eqs. (18)–(22), of its brief formulation Eq. (53). The analysis of the self-consistency algorithms starts with some definitions. The following operator K associates to a trial input density, $\rho^{\rm in}$, an output density, $\rho_n^{\rm out}$,

$$\rho^{\rm out} = K[\rho^{\rm in}] \triangleq \rho^{\rm v}[v[\rho^{\rm in}]]. \tag{54}$$

The discrepancy between the output and input densities,

$$R[\rho^{\rm in}] \triangleq \rho^{\rm out} - \rho^{\rm in} = K[\rho^{\rm in}] - \rho^{\rm in}, \tag{55}$$

is usually referred as the density residual. Such density residual vanish at the fixed point. Iteratively, one starts from a guess input density, computes the output density and the corresponding residual, then goes to the next step with a better input density, etc. The vast majority of algorithms to solve this self-consistency problem rely on the knowledge of pairs of trial density and corresponding density residual, to infer the next trial density. The easiest algorithm to implement, simple mixing, is defined at step n by

$$\rho_{n+1}^{\rm in} = \rho_n^{\rm in} + \lambda R[\rho_n^{\rm in}], \tag{56}$$

with λ being a tunable parameter, describing the incorporation of a fraction of the residual in the input density. If $\lambda = 1$, the output density is simply taken as the new input density. Most sophisticated algorithms take advantage of the history (at least the most recent part of it), and possibly include some preconditioning operator P, even varying at each step,

$$\rho_{n+1}^{\rm in} = \rho_n^{\rm in} + P_n \sum_{j=1}^{n} \lambda_j R[\rho_j^{\rm in}], \tag{57}$$

where the set of λ_j parameters and the possible preconditioners P_n are computed on the flight from the history, and differ for different algorithms.

Instead of such density-based mixing approaches, potential-based mixing approaches have also been proposed [39]. In order to distinguish the (non-linear) operators appearing in this potential-based approach from those appearing in the density-based approach (namely K, R and P), they are labeled with a "v" superscript. In the potential-based approaches, instead of Eqs. (53)– (57), one relies on

$$v^* = v[\rho^{\rm v}[v^*]], \tag{58}$$

$$v_n^{\rm out} = K^{\rm v}[v_n^{\rm in}] \triangleq v[\rho^{\rm v}[v_n^{\rm in}]], \tag{59}$$

$$R^{\rm v}[v_n^{\rm in}] \triangleq v_n^{\rm out} - v_n^{\rm in} = K^{\rm v}[v_n^{\rm in}] - v_n^{\rm in}, \tag{60}$$

$$v_{n+1}^{\rm in} = v_n^{\rm in} + P_n^{\rm v} \sum_{j=1}^{n} \lambda_j R^{\rm v}[v_j^{\rm in}]. \tag{61}$$

The density- and potential-mixing approaches are dual of each other: in the case of usual (unconstrained) DFT, for each density-based mixing algorithm, there exists an equivalent potential-based mixing algorithm in which the pairs of density and corresponding density residual are replaced by pairs of potential and corresponding potential residual.
Focusing on the potential-based approach, the self-consistent electronic energy expression, is now formulated as a minimization problem in the space of trial screened potentials, as follows,

$$E^{\rm SC}_{v_{\rm ext}} = \min_u E^{\rm v}_{v_{\rm ext}}[u] \tag{62}$$

with

$$E^{\rm v}_{v_{\rm ext}}[u] = T[\{\phi_{i,u}\}] + \int \rho^{\rm v}[u](\mathbf{r}) v_{\rm ext}(\mathbf{r}) d\mathbf{r} + E_{\rm Hxc}[\rho^{\rm v}[u]]. \tag{63}$$

The gradient of this functional of the potential has been computed in Ref. [42],

$$\frac{\delta E^{\rm v}_{v_{\rm ext}}[u]}{\delta u(\mathbf{r})} = \int \frac{\delta \rho^{\rm v}[u](\mathbf{r}')}{\delta u(\mathbf{r})} \left(K^{\rm v}[u](\mathbf{r}') - u(\mathbf{r}') \right) d\mathbf{r}' = \int \chi_0(\mathbf{r},\mathbf{r}') R^{\rm v}[u](\mathbf{r}')\, d\mathbf{r}'. \tag{64}$$

where the independent-particle susceptibility $\chi_0(\mathbf{r},\mathbf{r}')$ is to be evaluated at the screened potential u. This gradient obviously vanishes at the minimum, since $R^{\rm v}[v^*]$ vanishes. In practice, multiplication by χ_0^{-1}, like in Ref. [42], delivers a preconditioned gradient, which is nothing else than the residual $R^{\rm v}[u]$, so that $\chi_0(\mathbf{r},\mathbf{r}')$ does not even have to be computed. Hence, this approach shows that the usual potential-based self-consistency algorithms, Eq. (61) can be understood as mixing the preconditioned potential gradients of the electronic energy Eq. (63) from the current and previous steps.

3 Constrained density-functional theory: formalism and approximations

Ordinary DFT has the aim to compute the ground-state total energy and corresponding density/magnetization of a system of electrons placed in the potential of nuclei with known, fixed positions. Constrained DFT can enlarge the scope of ordinary DFT: for the same set of nuclei with known positions, the characterization of low-lying excited states or a superposition thereof is usually of great interest, and accessible by cDFT. With constraints, the system will usually not be in its ground state, but in a physically relevant state anyhow, or in a mixture of physically relevant states. Moreover, there is considerable freedom in the type of constraint that can be applied to explore such low-lying excited states. I will distinguish between the treatment of constraints that can be addressed at the Hohenberg-Kohn level, namely, those that are formulated in terms of the density and magnetization, or in terms of the correlated wavefunction (e.g. symmetry-constrained wavefunction), from those that are formulated in terms of quantities that are defined only at the Kohn-Sham level, e.g., that depend on the KS eigenenergies or the KS wavefunctions. For the first type of constraints, there exist analogs of the Hohenberg-Kohn theorems, based on the constrained-search strategy: the knowledge of an adequate exchange-correlation functional would deliver the exact energy under constraint.

3.1 Formal constrained density-functional theory

At the most fundamental level, constrained DFT can be formulated within the Hohenberg-Kohn framework by restricting the domain of the variational problem. This amounts to extending the Levy constrained-search formulation by imposing additional conditions on the admissible wavefunctions or densities.

Let $\hat{O}_I$ denote a set of observables (for example, symmetry operators, fragment charges, or local magnetizations, see the next subsection), and let N_I be the target values of their expectation values. The subscript I runs from 1 to the total number of constraints $I_{\max}$. One defines a constrained universal functional as

$$F^{\{N_I\}}[\rho_{\alpha\beta}] = \min_{\substack{\Psi\to\rho_{\alpha\beta} \\ \langle\Psi|\hat{O}_I|\Psi\rangle=N_I}} \big\langle \Psi \big| \hat{T} + \hat{V}_{ee} \big| \Psi \big\rangle. \tag{65}$$

The corresponding variational principle becomes

$$E^{\{N_I\}}_{v_{\text{ext}}}[\rho_{\alpha\beta}] = F^{\{N_I\}}[\rho_{\alpha\beta}] + \int \rho_{\alpha\beta}(\mathbf{r})\, v_{\text{ext},\beta\alpha}(\mathbf{r})\, d\mathbf{r}, \tag{66}$$

with

$$E^{\{N_I\}}_{v_{\text{ext}}} = \min_{\rho_{\alpha\beta}\to N} E^{\{N_I\}}_{v_{\text{ext}}}[\rho_{\alpha\beta}]. \tag{67}$$

This formulation is a direct generalization of the Levy constrained-search approach, Eq. (7), in which the minimization domain is further restricted. Eq.(67) delivers the lowest possible energy of the many-body Hamiltonian for a wavefunction that fulfills the constraints. It provides a formal justification for constrained DFT whenever the constraints can be expressed as expectation values of operators defined at the many-body level.

One can then pursue with the definition of an exchange-correlation functional, then the variational principle for the Kohn-Sham energy:

$$E^{\{N_I\}}_{\text{xc}}[\rho_{\alpha\beta}] = F^{\{N_I\}}[\rho_{\alpha\beta}] - T^{\{N_I\}}_{\text{s}}[\rho_{\alpha\beta}] - E_{\text{H}}[\rho]. \tag{68}$$

The energy functional is written as

$$E^{\{N_I\}}_{v_{\text{ext}}}[\rho_{\alpha\beta}] = T^{\{N_I\}}_{\text{s}}[\rho_{\alpha\beta}] + \int \rho_{\alpha\beta}(\mathbf{r})\, v_{\text{ext},\beta\alpha}(\mathbf{r})\, d\mathbf{r} + E_{\text{H}}[\rho] + E^{\{N_I\}}_{\text{xc}}[\rho_{\alpha\beta}]. \tag{69}$$

Note that the different functionals F, T_{s} and E_{xc} formally acquire a dependence on the constraints. They are not identical to the DFT functionals. Indeed, for example,

$$T^{\{N_I\}}_{\text{s}}[\rho_{\alpha\beta}] = \min_{\substack{\Psi\to\rho_{\alpha\beta} \\ \langle\Psi|\hat{O}_I|\Psi\rangle=N_I}} \langle \Psi | \hat{T} | \Psi \rangle, \tag{70}$$

compare with Eq. (14).

In principle, if the exact constrained functional $F^{\{N_I\}}[\rho_{\alpha\beta}]$ (or equivalently the associated exchange-correlation functional) were known, the corresponding constrained energy would be obtained exactly. In practice, however, one uses the same approximate functionals as in ordinary DFT, which makes cDFT an approximate albeit powerful method to access low-lying excited states.

3.2 Constraints at the Hohenberg-Kohn level

Constrained DFT was introduced in 1984 by Dederichs *et al.* [8]. Their first example of a constraint was the charge contained in a given volume V,

$$C_V[\rho] = \int_V \rho(\mathbf{r})\, d\mathbf{r}. \tag{71}$$

Many examples of constraints of this type can be constructed in a unified way using suitable weight functions in real space. In general, such constraints are written as

$$C_I[\rho_{\alpha\beta}] = \int w_{I,\alpha\beta}(\mathbf{r})\, \rho_{\beta\alpha}(\mathbf{r})\, d\mathbf{r}, \tag{72}$$

where the weights $w_{I,\alpha\beta}(\mathbf{r})$ define the observable of interest.
A natural generalization of Eq. (71) is obtained by partitioning the system into fragments A, B,..., each associated with a weight function $w_I(\mathbf{r})$. The corresponding fragment charge is defined as

$$C_I[\rho] = \int w_I(\mathbf{r})\, \rho(\mathbf{r})\, d\mathbf{r}. \tag{73}$$

Such constraints allow one to enforce a given charge distribution for each fragment, with the sum of the charges over all fragments being the total number of electrons N, which is essential for the description of charge-transfer states or diabatic states.
Several families of weight functions are commonly used in practice [8, 4, 28, 30].

- *Characteristic (step) functions.* The simplest choice consists in partitioning space into non-overlapping regions Ω_A, and defining

$$w_A(\mathbf{r}) = \begin{cases} 1 & \mathbf{r} \in \Omega_A, \\ 0 & \text{otherwise.} \end{cases} \tag{74}$$

  This choice directly corresponds to the original formulation of Dederichs *et al.*, and is conceptually simple. However, the resulting potentials are discontinuous at the boundaries, which may lead to numerical difficulties.

- *Smooth spherical functions.* In this case, each weight function $w_{\text{rad}}\big(|\mathbf{r}_\kappa|\big)$ is centered around an atom κ, and depends only on the distance with respect to that atom, $\mathbf{r}_\kappa \triangleq \mathbf{r} - \boldsymbol{\tau}_\kappa$. The radial weight function $w_{\text{rad}}(r)$ is equal to 1 for r smaller than some cut-off radius r_{c1}, decreases smoothly beyond that radius, and becomes exactly zero beyond some other cut-off radius r_{c2}. An alternative formulation, more convenient for numerical evaluation uses

$$w_A(\mathbf{r}) = w_{\text{rad2}}\big(\mathbf{r}_\kappa^2\big), \tag{75}$$

  with the following obvious relation $w_{\text{rad}}(t^{1/2}) = w_{\text{rad2}}(t)$.

  However, using such smooth spherical functions, one cannot partition the whole space, and hence the total charge in fragments each attached to one atom. In the case of magnetization, still, this is not a big problem, since most of the relevant magnetization is localized in small atom-centered regions, while the magnetization is small in the interatomic zone.

- *Smooth real-space partitioning functions.* In order to avoid discontinuities while partitioning the space, one often introduces smooth weight functions satisfying for every point in space

$$\sum_I w_I(\mathbf{r}) = 1, \tag{76}$$

with the weight functions $w_I(\mathbf{r})$ varying continuously in space. The charge at every point in space is partitioned among the close atoms. Examples include partitionings based on atomic-centered functions leading to smooth interpolation between regions.

- *Density-based (promolecule) weights.* As a subclass of the latter, weights can be defined using reference atomic (spherical) or fragment densities $\rho_A^{(0)}(\mathbf{r})$, called "promolecules" as

$$w_A(\mathbf{r}) = \frac{\rho_A^{(0)}(\mathbf{r})}{\sum_I \rho_I^{(0)}(\mathbf{r})}. \tag{77}$$

Such definitions ensure that the partitioning follows the chemical environment and adapts to the spatial distribution of the density.

In spin-dependent DFT, one can similarly constrain the magnetization associated with a fragment A, using in the collinear case,

$$C_A[\rho_{\alpha\beta}] = \int w_A(\mathbf{r}) \left(\rho^{\uparrow}(\mathbf{r}) - \rho^{\downarrow}(\mathbf{r})\right) d\mathbf{r}, \tag{78}$$

or, in the non-collinear case,

$$\mathbf{C}_A[\rho_{\alpha\beta}] = \int w_A(\mathbf{r})\, \mathbf{m}(\mathbf{r})\, d\mathbf{r}. \tag{79}$$

These constraints are widely used to fix local magnetic moments or their orientation, and to extract magnetic coupling parameters.
Beyond fixing the magnitude of the local magnetization, it is often desirable to only constrain its direction, while its magnitude is allowed to vary. Let $\mathbf{n}_A$ be a unit vector specifying the desired direction of the magnetization. A constraint fixing the direction of $\mathbf{C}_A$ can then be formulated by imposing that its component orthogonal to $\mathbf{n}_A$ vanishes

$$\mathbf{n}_A \times \mathbf{C}_A[\rho_{\alpha\beta}] = \mathbf{0}. \tag{80}$$

Equivalently, one may require that

$$\mathbf{C}_A[\rho_{\alpha\beta}] = C_A\, \mathbf{n}_A, \tag{81}$$

where C_A is left free.
More generally, any observable that can be expressed as a linear functional of the density or spin-density matrix can serve as a constraint. This includes, for example, spatial multipole moments of the density,

$$C_A[\rho] = \int w_A(\mathbf{r})\, r^l Y_{lm}(\hat{\mathbf{r}})\, \rho(\mathbf{r})\, d\mathbf{r}, \tag{82}$$

for the multipoles centered on the origin.

All these constraints share a common structure: they are linear functionals of $\rho_{\alpha\beta}$ and can therefore be incorporated within the Hohenberg-Kohn framework without leaving the density-based formalism. They define a restricted variational space corresponding to fixed values of selected collective variables, and thus provide access to a family of states beyond the ground state.

In addition to the constraints based on the electronic charge and on the magnetization, the Hohenberg and Kohn results (followed by the Kohn and Sham ones) can be extended to the lowest-energy state within a given symmetry sector, as shown by Gunnarsson and Lundqvist [43]. In their approach, the admissible wavefunctions are restricted to those compatible with a set of commuting operators $\{\hat{O}_I\}$

$$\left[\hat{H},\, \hat{O}_I\right] = 0. \tag{83}$$

In this case, the wavefunction and the energy of the lowest state for the specified symmetry are functionals of the density (or spin-density), and a variational principle analogous to DFT holds (with formally modified F and E_{xc} functionals).

One can also introduce constraints targeting specific electronic subspaces, for example localized atomic-like orbitals (such as d or f manifolds). Provided such subspace is defined at the many-body wavefunction level (as well as the Kohn-Sham level), a cDFT formalism ensues. Denoting by $\rho_d(\mathbf{r})$ the contribution of a given subspace to the density, and relying on one of the weighting schemes previously defined, the associated constraint can be formulated as

$$C_d[\rho] = \int w(\mathbf{r})\, \rho_d(\mathbf{r})\, d\mathbf{r}. \tag{84}$$

Such constraints are closely related to the construction of effective Hubbard-like models and to the definition of interaction parameters.

3.3 Constrained density-functional theory at the Kohn-Sham level

One should emphasize that not all constraints can be formulated at the Hohenberg-Kohn level. Constraints involving explicitly Kohn-Sham quantities, such as orbital occupations or eigenvalues, or Kohn-Sham wavefunctions, have no direct many-body counterpart and are inherently tied to the auxiliary non-interacting system. These constraints fall outside the rigorous DFT framework and should be regarded as density-functional-inspired schemes rather than strict extensions of DFT.

By the way, constraining the occupation numbers of the Kohn-Sham wavefunctions gives a method identical to the well-known ΔSCF approach for computing the excited states of molecules. See Ref. [44] for an attempt to formulate the ΔSCF on a firm footing, this reference being also an entry point in the history of the ΔSCF method and its applications.

4 Constrained density-functional theory algorithms

The formal framework of constrained DFT, discussed in Sec. 3, does not by itself provide a practical prescription to enforce the constraints during the self-consistent solution of the Kohn-Sham equations. Algorithmic strategies must therefore be devised to impose the constraints while preserving numerical stability and convergence.

In this section, after framing the cDFT minimization problem in terms of Lagrange multipliers, I review the main approaches used in practice, emphasizing their underlying principles and their connection with standard self-consistent field (SCF) techniques.

Formally, the most direct way to impose constraints is through the introduction of Lagrange multipliers, following the original formulation of Dederichs *et al.* [8]. For a set of constraints $C_I[\rho_{\alpha\beta}] = N_I$, one defines the augmented functional

$$E_{v_{\text{ext}}}^{\{N_I\}+}[\rho_{\alpha\beta}, \{\lambda_I\}] = E_{v_{\text{ext}}}[\rho_{\alpha\beta}] + \sum_I \lambda_I \big(C_I[\rho_{\alpha\beta}] - N_I\big), \tag{85}$$

where λ_I are Lagrange multipliers. At the stationary point of $E_{v_{\text{ext}}}^{\{N_I\}+}$, one has

$$\frac{\delta E_{v_{\text{ext}}}^{\{N_I\}+}}{\delta \rho_{\alpha\beta}} = 0, \qquad C_I[\rho_{\alpha\beta}] = N_I, \tag{86}$$

which ensures that the constraints are exactly satisfied.

In the case of generic constraints of the type Eq. (72), the Euler-Lagrange equations lead to modified Kohn-Sham equations where the effective potential is augmented by a constraining contribution,

$$v_{\alpha\beta}(\mathbf{r}) \longrightarrow v_{\alpha\beta}(\mathbf{r}) + \sum_I \lambda_I \, w_{I,\beta\alpha}(\mathbf{r}). \tag{87}$$

Within this formulation, the constrained ground-state energy corresponds to a saddle point (minimax problem),

$$E_{v_{\text{ext}}}^{\{N_I\}+} = \min_{\rho_{\alpha\beta}} \max_{\{\lambda_I\}} E_{v_{\text{ext}}}^{\{N_I\}+}[\rho_{\alpha\beta}, \{\lambda_I\}], \tag{88}$$

i.e., a minimization with respect to the density and a maximization with respect to the Lagrange multipliers [4].

4.1 Microiterations

A practical implementation of the Lagrange-multiplier method requires the simultaneous determination of the density (or wavefunctions) and of the multipliers $\{\lambda_I\}$. A possible strategy is based on nested iterative loops, often referred to as *microiterations* [4].

In this approach, one distinguishes: (1) an *outer loop*, in which the Kohn-Sham equations are solved self-consistently; (2) an *inner loop* (microiterations), in which the multipliers are updated so as to enforce the constraints.

The outer loop closely resembles a normal DFT calculation, with SCF iterations being performed to optimize the KS wavefunctions. Within each step of the outer loop, a second loop of

microiterations is performed to determine the Lagrange multipliers $\{\lambda_I\}$ that make the density satisfy the charge and spin constraints. After the first few iterations of the outer loop, it is common for the inner loop to converge after only two or three microiterations. While conceptually simple, this nested-loop structure may be computationally demanding. By the way, the reverse ordering might be possible: having an inner loop to determine density and wavefunctions for fixed Lagrange multipliers $\{\lambda_I\}$, while the outer loop involves a multi-dimensional search in the space of Lagrange parameters.

4.2 Penalty function approaches

An alternative to the Lagrange multiplier method consists in replacing the linear constraint term by a quadratic penalty function. The constrained energy functional is then written as

$$E_{v_{\text{ext}}}^{\{N_I\}\text{pen}}[\rho_{\alpha\beta}] = E_{v_{\text{ext}}}[\rho_{\alpha\beta}] + \sum_I \frac{\kappa_I}{2}\big(C_I[\rho_{\alpha\beta}]-N_I\big)^2, \tag{89}$$

where κ_I are penalty parameters.

This approach eliminates the need for auxiliary variables (the λ_I), and reduces the constrained optimization problem to a standard minimization. However, the constraints are only satisfied approximately, and enforcement becomes exact only in the limit $\kappa_I \to \infty$.

Penalty-based formulations are used in several practical implementations, including constrained non-collinear magnetism [28]. Indeed, in that work, the additional term added to the energy is quadratic in the deviation from the target configuration (see, e.g., Eq. (A.2) of Ref. [28]), which corresponds to a penalty functional rather than a Lagrange-multiplier formulation. Indeed, the added term scales as $(C_I-N_I)^2$, not linearly in (C_I-N_I), and therefore does not enforce the constraint exactly at finite parameter values.

An important property of such schemes is that the penalty contribution to the energy vanishes as the constraint is satisfied. In particular, it can be shown that, near convergence,

$$E_{v_{\text{ext}}}^{\{N_I\}\text{pen}} - E_{v_{\text{ext}}}^{\{N_I\}+} \propto \frac{1}{\kappa_I}, \tag{90}$$

so that increasing κ_I improves the accuracy of the constraint at the expense of numerical stiffness, with associated difficulties to converge.

More recently, Royo and Stengel [29] have shown that the apparent limitations of penalty-function approaches can be overcome by exploiting exact Legendre-transform relations between different functionals. In their framework, the penalty functional Eq. (89) is interpreted as a convenient auxiliary functional, whose constrained variables (e.g. target moments) play the role of independent parameters. The physically relevant quantities, corresponding to the exact Lagrange-multiplier formulation, can then be recovered *a posteriori* from the penalty-based results via simple linear-algebra operations involving response matrices. In particular, second derivatives of the penalty functional yield a "stiffened" response (with improved numerical conditioning), which can be exactly transformed into the true constrained response associated with the variational principle of Eq. (85). This procedure establishes a one-to-one mapping between

penalty-function and Lagrange-multiplier approaches, demonstrating their formal equivalence at the level of observables. In addition to providing a practical route to accurate constrained calculations, this result justifies the use of penalty functionals as efficient preconditioners, combining numerical robustness with exact enforcement of the constraints after post-processing.

4.3 Lagrange multipliers again: a potential-based SCF approach

The potential-based SCF formulation introduced in Sec. 2.4, see Eqs. (58)–(64), can be extended to constrained problems by incorporating Lagrange multipliers directly into the potential-dependent energy functional [30]. A key advantage of this formulation is that it preserves the structure of the SCF problem, allowing one to reuse without modifications the algorithms developed for unconstrained DFT. In the present subsection, this approach is described for an electronic density single constraint; its extension to multiple spin-dependent constraints is discussed in Ref. [30].

For a single constraint $C_{\rm A}[\rho] = N_{\rm A}$, the augmented functional takes the form

$$E^{\rm v+}_{v_{\rm ext},N_{\rm A}}[u,\Lambda] = E^{\rm v}_{v_{\rm ext}}[u] + \Lambda\big(\rho^{\rm v}_{\rm A}[u] - N_{\rm A}\big), \tag{91}$$

where I introduce the shorthand notation

$$\rho^{\rm v}_{\rm A}[u] \equiv C_{\rm A}[\rho^{\rm v}[u]], \tag{92}$$

and Λ is the associated Lagrange multiplier.

For a fixed value of Λ, the constrained problem reduces to a standard minimization with respect to the trial potential,

$$E^{+}_{v_{\rm ext},N_{\rm A}}[\Lambda] = \min_{u} E^{\rm v+}_{v_{\rm ext},N_{\rm A}}[u,\Lambda]. \tag{93}$$

The gradient of $E^{\rm v}_{v_{\rm ext}}[u]$ with respect to the potential is given by Eq. (64). Applying the same derivation to the augmented functional leads to

$$\frac{\delta E^{\rm v+}_{v_{\rm ext},N_{\rm A}}[u,\Lambda]}{\delta u(\mathbf{r})} = \int \chi_0(\mathbf{r},\mathbf{r}')\, R^{\rm v+}(\mathbf{r}')\, d\mathbf{r}', \tag{94}$$

where the modified residual is defined as

$$R^{\rm v+}(\mathbf{r}) = R^{\rm v}(\mathbf{r}) + \Lambda\, w_{\rm A}(\mathbf{r}). \tag{95}$$

From Eqs. (93) and (94), the self-consistent solution corresponds to a potential $u = v^*$ satisfying

$$0 = R^{\rm v+}(\mathbf{r}) = v_{\rm out}(\mathbf{r}) - v^*(\mathbf{r}) + \Lambda w_{\rm A}(\mathbf{r}), \tag{96}$$

for all $\mathbf{r}$. Thus, the self-consistent condition can be interpreted as the requirement that the difference between output and input potentials lies entirely in the subspace spanned by the weight function $w_{\rm A}$, with proportionality factor Λ.

An explicit expression for the Lagrange multiplier is obtained by projecting Eq. (96) onto $w_{\rm A}$,

$$\Lambda = -R^{\rm v}_{\rm A}[v^*]\,(W_{\rm AA})^{-1}, \tag{97}$$

where

$$R^{\mathrm{v}}_{\mathrm{A}}[u] = \int R^{\mathrm{v}}(\mathbf{r}) w_{\mathrm{A}}(\mathbf{r})\, d\mathbf{r}, \tag{98}$$

and

$$W_{\mathrm{AA}} = \int w_{\mathrm{A}}(\mathbf{r}) w_{\mathrm{A}}(\mathbf{r})\, d\mathbf{r}. \tag{99}$$

This result provides a direct and explicit determination of the Lagrange multiplier from the potential residual. This feature is specific to the potential-based formulation and contrasts with wavefunction- or density-based approaches, where the multiplier must typically be determined through an additional iterative procedure.

Going one step further, the dependence on Λ can be eliminated by inserting Eq. (97) back into the functional. Evaluating Λ at a general u leads to the definition of the functional

$$E^{\mathrm{cDFT}}_{v_{\mathrm{ext}},N_{\mathrm{A}}}[u] = E^{\mathrm{v}}_{v_{\mathrm{ext}}}[u] - R^{\mathrm{v}}_{\mathrm{A}}[u]\,(W_{\mathrm{AA}})^{-1}\big(\rho^{\mathrm{v}}_{\mathrm{A}}[u]-N_{\mathrm{A}}\big). \tag{100}$$

This functional depends only on the potential u, while both v_{ext} and N_{A} appear as external parameters on an equal footing. By construction, it yields the constrained ground-state energy when evaluated at the self-consistent potential,

$$E^{\mathrm{SC}}_{v_{\mathrm{ext}},N_{\mathrm{A}}} = E^{\mathrm{cDFT}}_{v_{\mathrm{ext}},N_{\mathrm{A}}}[v^*], \tag{101}$$

and is stationary with respect to variations of u around v^*,

$$E^{\mathrm{cDFT}}_{v_{\mathrm{ext}},N_{\mathrm{A}}}[u] = E^{\mathrm{cDFT}}_{v_{\mathrm{ext}},N_{\mathrm{A}}}[v^*] + \mathcal{O}\big((u-v^*)^2\big). \tag{102}$$

The corresponding functional derivative reads

$$\frac{\delta E^{\mathrm{cDFT}}_{v_{\mathrm{ext}},N_{\mathrm{A}}}[u]}{\delta u(\mathbf{r})} = \int \chi_0(\mathbf{r},\mathbf{r}') R^{\mathrm{v}+}\mathbf{r}' d\mathbf{r}' + \left(\int \epsilon_e(\mathbf{r},\mathbf{r}') w_{\mathrm{A}}(\mathbf{r}') d\mathbf{r}'\right)(W_{\mathrm{AA}})^{-1}\big(\rho^{\mathrm{v}}_{\mathrm{A}}[u]-N_{\mathrm{A}}\big), \tag{103}$$

with

$$\Lambda_{\mathrm{A}}[u] = -R^{\mathrm{v}}_{\mathrm{A}}[u](W_{\mathrm{AA}})^{-1}, \tag{104}$$

and where $\epsilon_e(\mathbf{r},\mathbf{r}')$ is the electron dielectric response function [42, 30].

At self-consistency, both $R^{\mathrm{v}+}[v^*, \Lambda_{\mathrm{A}}[v^*]]$ and $\rho^{\mathrm{v}}_{\mathrm{A}}[v^*]-N_{\mathrm{A}}$ vanish, which confirms the stationary character of the functional.

An important property of $\Lambda_{\mathrm{A}}[u]$ is that it enforces the orthogonality condition

$$\int R^{\mathrm{v}+}(\mathbf{r}) w_{\mathrm{A}}(\mathbf{r})\, d\mathbf{r} = 0, \tag{105}$$

i.e., it removes the component of the residual along the constraint direction.

This naturally motivates the introduction of a modified residual adapted to constrained DFT,

$$R^{\mathrm{cDFT}}(\mathbf{r}) = R^{\mathrm{v}+}(\mathbf{r}) + c\, w_{\mathrm{A}}(\mathbf{r})\big(\rho^{\mathrm{v}}_{\mathrm{A}}[u]-N_{\mathrm{A}}\big),$$

where c is a numerical parameter of order unity.

Since the two contributions to this modified residual belong to orthogonal subspaces, the condition $R^{\mathrm{cDFT}}[u] = 0$ ensures simultaneously the fulfillment of the SCF condition and of the constraint. This formulation provides a direct route to extend standard potential-based SCF algorithms to constrained DFT calculations.

5 Some applications of constrained density-functional theory

The computation of the Hubbard U for use in DMFT. Following Cococcioni and de Gironcoli [7], an important application of constrained density-functional theory is the determination of effective interaction parameters entering low-energy many-body models, such as the U parameter in the Hubbard model or extensions thereof, see e.g., Ref. [5, 45], used in DFT+DMFT approaches. In this formulation based on constrained DFT and linear-response theory, U is computed in a fully first-principles and internally consistent manner. The key idea is to evaluate the curvature of the total energy with respect to variations of the occupation of a localized orbital subspace associated with a given atomic site.

In this framework, one considers the total energy as a functional of constrained occupations $\{q_I\}$ of localized orbitals,

$$E[\{q_I\}] = \min_{\{\phi_i\}\to N} \left\{ T_{\rm s}[\{\phi_i\}] + \int \rho[\{\phi_i\}](\mathbf{r})\, v_{\rm ext}(\mathbf{r})\, d\mathbf{r} + E_{\rm Hxc}[\rho[\{\phi_i\}]] + \sum_I \Lambda_I \big(n_I[\{\phi_i\}] - q_I\big) \right\}, \tag{106}$$

where n_I denotes the occupation of the localized manifold on site I, and Λ_I are Lagrange multipliers enforcing the constraint. The Hubbard interaction is then defined, with respect to the non-self-consistent non-interacting Hamiltonian, as the curvature of the interacting energy with respect to the occupation of a given site,

$$U = \frac{\partial^2 E[\{q_I\}]}{\partial q_I^2}\,, \tag{107}$$

evaluated at the ground-state occupation.

However, in the DFT case, this curvature contains mean-field contributions that are not related to explicit electron-electron interactions, but that appear in the Kohn-Sham treatment. To isolate the physically meaningful interaction, the same construction is applied to the Kohn-Sham energy,

$$E_{\rm KS}[\{q_I\}] = \min_{\{\phi_i\}\to N} \left\{ T_{\rm s}[\{\phi_i\}] + \int \rho[\{\phi_i\}](\mathbf{r})\, v_{\rm KS}(\mathbf{r})\, d\mathbf{r} + \sum_I \Lambda_I^{\rm KS} \big(n_I[\{\phi_i\}] - q_I\big) \right\}, \tag{108}$$

where $v_{\rm KS}$ is kept frozen to the one of the non-constrained DFT case. The effective Hubbard parameter is defined as the difference between the interacting and non-interacting curvatures,

$$U = \frac{\partial^2 E[\{q_I\}]}{\partial q_I^2} - \frac{\partial^2 E_{\rm KS}[\{q_I\}]}{\partial q_I^2}\,. \tag{109}$$

A key simplification arises from the observation that the derivatives of the energy with respect to occupations can be expressed in terms of the Lagrange multipliers,

$$\frac{\partial E}{\partial q_I} = -\Lambda_I, \qquad \frac{\partial^2 E}{\partial q_I^2} = -\frac{\partial \Lambda_I}{\partial q_I}, \tag{110}$$

and similarly for the Kohn-Sham system. This allows one to rewrite Eq. (109) as

$$U = \frac{\partial \Lambda_I^{\rm KS}}{\partial q_I} - \frac{\partial \Lambda_I}{\partial q_I}. \tag{111}$$

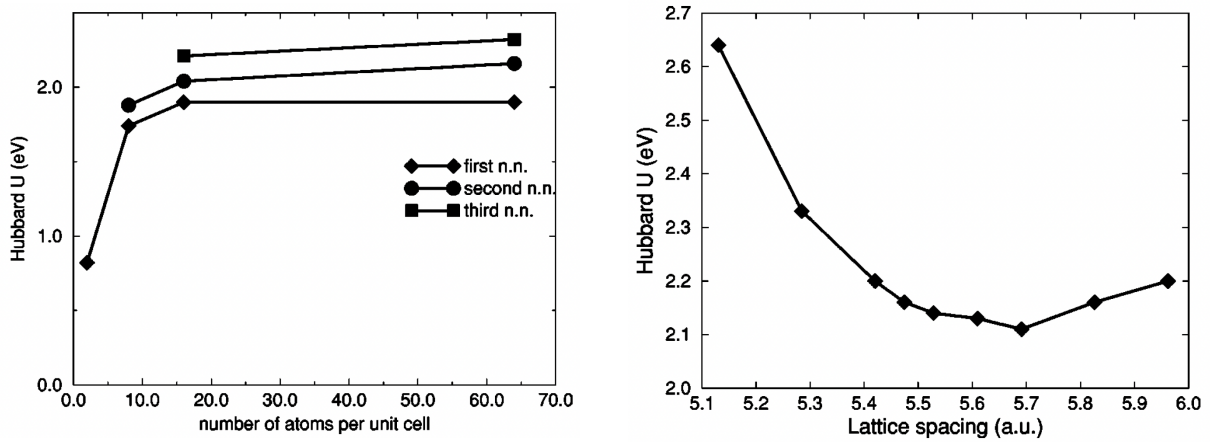

Fig. 1: *(Left) Calculated Hubbard U in metallic iron for different supercells. Lines connect results from the cell-extrapolation procedure and different symbols correspond to inclusion of screening contributions up to the indicated shell of (nearest-)neighbors of the perturbed atom. (Right) Lattice spacing dependence of the calculated Hubbard U parameter for iron. Reprinted figures from Ref. [7] with permission. Copyright ©2005 The Americal Physical Society.*

In practice, it is more convenient to perform a Legendre transform and work with the Lagrange multipliers as independent variables. In this representation, the perturbation induced by Λ_I corresponds to a shift of the local potential acting on the selected subspace,

$$\Delta v(\mathbf{r}) = \sum_I \Lambda_I \, P_I, \tag{112}$$

where P_I is the projector onto the localized orbitals of site I.
One then introduces the interacting and non-interacting response matrices

$$\chi_{IJ} = \frac{\partial n_I}{\partial \Lambda_J}, \qquad \chi^0_{IJ} = \frac{\partial n_I}{\partial \Lambda^{\mathrm{KS}}_J}, \tag{113}$$

which describe how localized occupations respond to local potential shifts.
Within this linear-response framework, the effective Hubbard interaction is obtained as

$$U = \left(\chi_0^{-1} - \chi^{-1}\right)_{II}, \tag{114}$$

which highlights the screening effects due to the electronic environment. This expression is formally analogous to a screened interaction in linear-response theory, where χ^0 represents the bare (non-interacting) response and χ the fully screened one.
The resulting values of U can then be used in DFT+U or DFT+DMFT calculations, establishing a rigorous connection between first-principles electronic structure methods and many-body model Hamiltonians.
In practical calculations, the response functions are evaluated numerically by applying small local perturbations to the Kohn-Sham potential and monitoring the changes in the occupations of the localized orbitals. Importantly, the screening is computed within supercells of increasing size, without artificially decoupling the localized subspace, ensuring a realistic description of the environment.

The convergence of the computed Hubbard interaction with respect to the spatial extent of the screening can be illustrated using the case of metallic iron, as shown in the left side of Fig. 1. The effective interaction parameter U is obtained from the linear-response expression Eq. (114), and depends on the range of the induced charge redistribution following a local perturbation. By including progressively larger coordination shells in the response functions, one observes that the value of U converges, reflecting the degree of spatial delocalization of the screening charge. In metallic systems such as iron, screening is relatively long ranged, and contributions from several coordination shells are required to obtain a quantitatively accurate value of U. On the right side of Fig. 1, the dependence of U on the lattice parameter of Fe (e.g. for different pressures) is shown. This behavior highlights the importance of treating screening within the full crystal environment, rather than within an artificially localized or atomic picture.

Constraining the direction of local magnetization in BCC Fe. I now turn to a representative application of cDFT to explore the energy landscape as a function of local spin magnetizations in addition to the more usual DFT variables like atomic positions and lattice parameters. In this application, I consider body-centered cubic (bcc) iron, using a two-atom conventional cell, in which the directions of local magnetization vectors on each sublattice are independently controlled [30]. In this setup, the angle between the magnetization vectors of the two sublattices is continuously varied from the ferromagnetic configuration ($0°$) to the antiferromagnetic configuration ($180°$), without constraining the magnetization vector length, that is determined self-consistently to minimize the energy.

The resulting dependence of the total energy and local magnetic moment on the spin angle is shown in the left column of Fig. 2. The calculated energy variation from different methodologies, including the potential-based self-consistent algorithm, agree reasonably well, for both LDA and GGA(PBE) functionals. The magnitude of the local magnetization decreases as the angle between neighboring spins increases, reflecting the gradual destabilization of the ferromagnetic alignment. Interestingly, the evolution of the magnetic moment as a function of the spin angle is not perfectly smooth, but instead exhibits small irregularities despite the high numerical precision achieved in the calculations. This behavior is attributed to non-smooth changes in the electronic density of states, in particular the presence of Van Hove critical points, that shift as the spin configuration evolves.

Beyond such validation step, the potential-based SCF method enables the investigation of magnetoelastic coupling by analyzing the response of the stress tensor to changes in the magnetic configuration. When the lattice parameter is kept fixed, the rotation of the magnetic moments induces significant variations in the stress, which can be conveniently characterized through the pressure (the trace of the stress tensor). As shown in the top right panel of Fig. 2, the pressure varies over a wide range, reaching amplitudes of the order of 8–12 GPa depending on the exchange-correlation functional used. This variation is substantial when compared to the bulk modulus of iron, highlighting the strong coupling between magnetic order and mechanical properties.

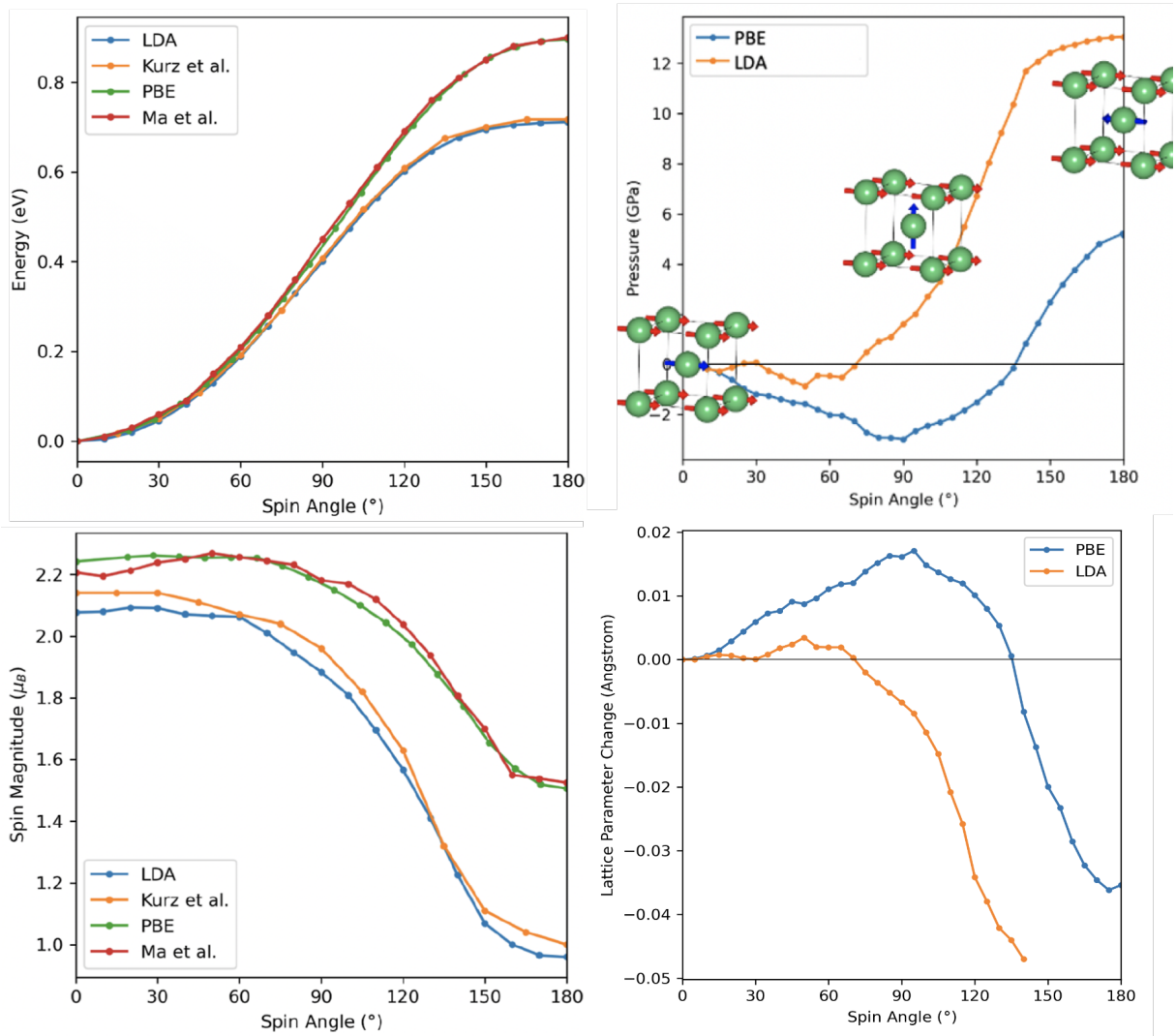

Fig. 2: *Energy (top, left), pressure (top, right), spin magnitude (bottom, left) and relaxed lattice parameter (bottom, right), as a function of the spin angle between the two sublattices in a Fe BCC conventional cell. The top right figure also illustrates the relative angle between the two spin sublattices. LDA data (blue) from Ref. [30] are compared to those from Kurz et al. [46] (orange), while GGA(PBE) data (green) from Ref. [30] are compared to those of Ma and Dudarev [28] (red). Reproduced from Ref. [30] with permission. Copyright ©2022 The Authors. Published by the American Chemical Society.*

Allowing for structural relaxation at fixed spin angle further reveals the consequences of this coupling at the level of equilibrium geometry. For each imposed magnetic configuration, the lattice parameter can be optimized, yielding the results shown in the bottom right panel of Fig. 2. The evolution of the equilibrium lattice parameter closely follows the trends observed in the pressure, demonstrating consistency between the stress response and total-energy minimization. The magnitude of the lattice parameter variation reaches approximately 0.06 Å, corresponding to about 2% of the total lattice parameter, which is a sizable structural effect. As in the case of the magnetization, a slightly irregular dependence on the spin angle is observed, again reflecting subtle features in the electronic structure.

Altogether, this example demonstrates that the constrained DFT formalism allows one to treat magnetic degrees of freedom, structural parameters, and mechanical response on an equal footing. It provides direct access not only to the energy landscape associated with noncollinear magnetic configurations, but also to the associated stresses and equilibrium structures, thereby enabling a comprehensive characterization of magnetoelastic couplings within a unified first-principles approach. Such capabilities are essential for the construction of effective model Hamiltonians, second-principles methods, or machine-learning potentials that explicitly incorporate coupled spin and lattice degrees of freedom.

Electron-inertia-induced magnon mass within constrained DFPT. The perturbative version of cDFT gives the possibility to access, in a controlled and numerically stable manner, the nonadiabatic dynamics of spin degrees of freedom, including their coupling to lattice and electronic excitations. In this context, the recent work of Royo and Stengel (RS) [29] provides a remarkable advance by establishing a unified framework to compute the frequency-dependent response of noncollinear magnets under constrained magnetic moments, and by demonstrating the emergence of finite magnon inertia. In what follows, I summarize the main formal ingredients of this result, emphasize its connection to the constrained functional approach, and discuss its physical implications for spin dynamics.

A key conceptual step of the theory consists in performing a systematic expansion of the constrained functional in powers of frequency. The spin-phonon Hessian can be expressed as

$$U(\omega) = K + i\omega G - \omega^2 M + \cdots , \tag{115}$$

where K is the static (adiabatic) Hessian with respect to atomic displacements and local magnetization (that is, the matrix of interatomic force constants, spin susceptibilities and their adiabatic couplings), G is the Berry-curvature tensor governing precessional dynamics of spins, and M is a mass tensor arising at second order in frequency.

While the first two terms are familiar from adiabatic phonon and the semiclassical theory of magnons, the third term represents a genuine nonadiabatic correction. Crucially, the tensor M is not limited to ionic contributions in the phonon sector: it also contains an electronic component stemming from the frequency dispersion of the response functions.

When restricting the coupled atomic displacement – magnetization dynamical equation to the spin-spin sector, one obtains a generalized equation of motion for the local spin amplitudes

$$\sum_l M_{jl}\, \ddot{s}_l - G_{jl}\, \dot{s}_l + K_{jl}\, s_l = 0, \tag{116}$$

where j and l label atomic sites. This result represents a fundamental modification of the conventional Landau-Lifshitz dynamics [47]. Indeed, the RS formalism introduces a second-order inertial term proportional to $M\ddot{s}$. From a physical standpoint, this implies that magnons behave as particles with finite effective mass, rather than purely massless precessional modes.

The microscopic origin of this mass term is explicitly identified in the theory [29]: the additional contribution arises from “the inertia of the electrons that are dragged by a given degree

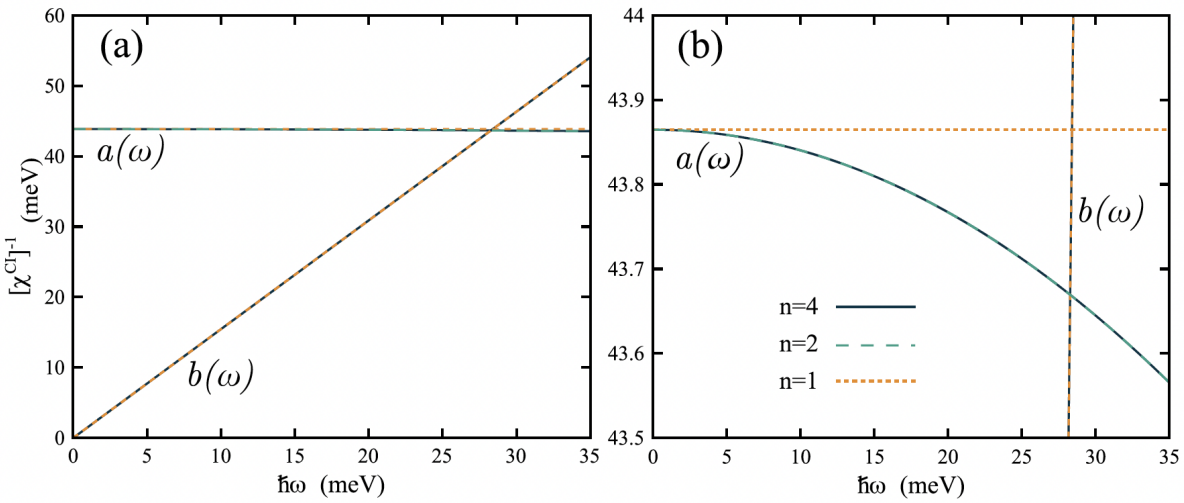

Fig. 3: *(a) Frequency dependence of the optical-magnon coefficients of Eq.* (117)*, as obtained from polynomial frequency interpolation at different degrees: n=4 (dark solid line), n=2 (turquoise dashed line), and n=1 (orange dashed line). (b) shows an amplified view of the abscissa axis around the intersection of the curves shown in (a). Reproduced from Royo and Stengel [29] under the terms of the Creative Commons Attribution 4.0 International (CC BY 4.0) license.*

of freedom along its trajectory". In other words, during spin precession, the electronic cloud cannot instantaneously follow the rotation of the local magnetization. The resulting delay produces an effective kinetic energy term, which manifests itself at second order in the frequency expansion.

Royo and Stengel examine the size of this correction in the case of ferromagnetic CrI_3, a van der Waals ferromagnet that remains spin-ordered down to the monolayer limit [48]. Its properties arise from the interplay of electronic, vibrational, and magnetic degrees of freedom. Magnon-phonon coupling has been treated with model Hamiltonians for this material [49].

Although small, the effect can be seen in the analysis of the optical magnon response. Royo and Stengel define

$$u_{\pm}(\omega) = a(\omega) \mp b(\omega) \approx K \mp \omega G - \omega^2 M + \cdots \tag{117}$$

The zeros of $u_{\pm}$ correspond to the magnon resonances. The "+" and "–" modes correspond to clockwise (+) and counterclockwise (-) spin precession.

Fig. 3 shows the frequency dependence of the coefficients entering the magnon propagator. In particular: the coefficient $b(\omega)$ is nearly linear in ω, consistent with the Berry-curvature term; the coefficient $a(\omega)$, however, exhibits a very small quadratic curvature which cannot be captured within the standard adiabatic approximation. At finite frequencies (e.g. THz regime), inertial effects may become significant and modify the propagation and damping of spin waves.

6 Conclusion

In this lecture, I have presented the formal foundations, algorithmic strategies, and selected applications of constrained density-functional theory (cDFT). Starting from the Hohenberg-Kohn framework and the Levy constrained-search formulation, I have shown that cDFT can be understood as a natural extension of density-functional theory in which the variational space is restricted to enforce physically meaningful conditions, such as fragment charges, local magnetizations, or symmetry constraints. This perspective provides a rigorous grounding for a wide range of practical methods that go beyond the standard ground-state description.

At the formal level, I have emphasized that constraints formulated in terms of (spin-)density functionals retain a strict connection with many-body quantum mechanics, whereas constraints defined at the Kohn-Sham level introduce additional approximations. In practice, however, both classes of approaches play an essential role in modern electronic-structure calculations, enabling access to excited-state properties, diabatic states, and effective model parameters.

On the algorithmic side, I have reviewed the main strategies used to enforce constraints, including the Lagrange-multiplier formulation with micro-iterations, penalty-function approaches, and the more recent development based on potential-based self-consistent schemes. The latter method exhibit the most straightforward connection between constrained and unconstrained DFT calculations. Recent advances have further shown that penalty-function methods can be improved, and considered as preconditioned versions of the constrained problem, with exact results recovered through appropriate transformations.

The applications discussed in this work illustrate several aspects of constrained DFT. In particular, I have highlighted its capability in the construction of effective Hamiltonians, such as the determination of Hubbard interaction parameters or magnetic exchange couplings, as well as its use in exploring complex energy landscapes involving coupled spin, charge, and structural degrees of freedom. The ability of cDFT to treat these variables on an equal footing makes it a powerful tool for bridging first-principles calculations and model-based descriptions of condensed matter systems.

A particularly interesting recent development in constrained density-functional theory, is the ability of cDFT to provide parameters to study the dynamical regime of models. In this framework, constraints not only improve the numerical stability of response calculations but also enable the systematic investigation of nonadiabatic effects. The emergence of an effective magnon mass associated with electron inertia provides a striking example of how constrained approaches can uncover subtle physical phenomena that are beyond the reach of traditional adiabatic theories, and calls for a refinement of established models such as the Landau-Lifshitz description of spin dynamics.

Looking forward, constrained DFT is expected to continue to play an important role in several areas of computational materials science and chemistry. These include the construction of accurate low-energy Hamiltonians for strongly correlated systems, the development of second-principles and machine-learning models incorporating electronic and magnetic degrees of freedom, and the investigation of ultrafast and non-equilibrium phenomena where coupled electronic, spin, and lattice dynamics are essential.

References

[1] R.M. Martin: *Electronic structure. Theory and practical methods.* (Cambridge University Press, Cambridge, 2004)

[2] F. Giustino: *Materials Modelling using Density Functional Theory* (Oxford University Press, 2014)

[3] A.M. Teale, T. Helgaker, and A. Savin, Phys. Chem. Chem. Phys. **24**, 28700 (2022)

[4] B. Kaduk, T. Kowalczyk, and T. Van Voorhis, Chem. Rev. **112**, 321 (2012)

[5] R.M. Martin, L. Reining, and D.M. Ceperley: *Interacting Electrons. Theory and Computational Approaches.* (Cambridge University Press, Cambridge, 2016)

[6] A. Georges, G. Kotliar, W. Krauth, and M.J. Rozenberg, Rev. Mod. Phys. **68**, 13 (1996)

[7] M. Cococcioni and S. de Gironcoli, Phys. Rev. B **71**, 035105 (2005)

[8] P.H. Dederichs, S. Blügel, R. Zeller, and H. Akai, Phys. Rev. Lett. **53**, 2512 (1984)

[9] R.A. Marcus, J. Chem. Phys. **24**, 966 (1956)

[10] R.A. Marcus and N. Sutin, Biochim. Biophys. Acta – Rev. Bioenerg. **811**, 265 (1985)

[11] S. Blundell: *Magnetism in Condensed Matter* (Oxford University Press, 2001)

[12] I. Dzyaloshinskii, J. Phys. Chem. Solids **4**, 241 (1958)

[13] T. Moriya, Phys. Rev. **120**, 91 (1960)

[14] H. Komatsu, Y. Nonomura, and M. Nishino, Phys. Rev. B **103**, 214404 (2021)

[15] R. Gebauer and S. Baroni, Phys. Rev. B **61**, R6459 (2000)

[16] D.M. Bylander, Q. Niu, and L. Kleinman, Phys. Rev. B **61**, R11875 (2000)

[17] P. Garcia-Fernandez, J.C. Wojdeł, J. Iniguez, and J. Junquera, Phys. Rev. B **93**, 195137 (2016)

[18] A.R. Damodaran, J.D. Clarkson, Z. Hong, H. Liu, A.K. Yadav, C.T. Nelson, S.-L. Hsu, M.R. McCarter, K.-D. Park, V. Kravtsov, A. Farhan, Y. Dong, Z. Cai, H. Zhou, P. Aguado-Puente, P. García-Fernández, J. Íñiguez, J. Junquera, A. Scholl, M.B. Raschke, L.-Q. Chen, D.D. Fong, R. Ramesh, and L. Martin, Nat. Mater. **16**, 1003 (2017)

[19] C. Escorihuela-Sayalero, J.C. Wojdeł, and J. Iniguez, Phys. Rev. B **95**, 094115 (2017)

[20] P. Shafer, P. García-Fernández, P. Aguado-Puente, A.R. Damodaran, A.K. Yadav, C.T. Nelson, S.-L. Hsu, J.C. Wojdeł, J. Íñiguez, L.W. Martin, E. Arenholz, J. Junquera, and R. Ramesh, Proc. Natl. Acad. Sci. USA **115**, 915 (2018)

[21] I. Novikov, B. Grabowski, F. Körmann, and A. Shapeev, npj Comput. Mater. **8**, 1 (2022)

[22] S. Nikolov, M. Wood, A. Cangi, J. Maillet, M. Marinica, A. Thompson, M. Desjarlais, and J. Tranchida, npj Comput. Mater. **7**, 1 (2021)

[23] M. Eckhoff and J. Behler, npj Comput. Mater. **7**, 1 (2021)

[24] R. Drautz, Phys. Rev. B **102**, 024104 (2020)

[25] M. Melander, E. Ö. Jónsson, J.J. Mortensen, T. Vegge, and J.M.G. Lastra, J. Chem. Theory Comput. **12**, 5367 (2016)

[26] O. Hegde, M. Grabowski, X. Zhang, O. Waseda, T. Hickel, C. Freysoldt, and J. Neugebauer, Phys. Rev. B **102**, 144101 (2020)

[27] Q. Wu and T. Van Voorhis, J. Chem. Theory Comput. **2**, 765 (2006)

[28] P.-W. Ma and S.L. Dudarev, Phys. Rev. B **91**, 054420 (2015)

[29] M. Royo and M. Stengel, Phys. Rev. X **16**, 011049 (2026)

[30] X. Gonze, B. Seddon, J. Elliott, C. Tantardini, and A. Shapeev, J. Chem. Theory Comput. **18**, 6099 (2022)

[31] P. Hohenberg and W. Kohn, Phys. Rev. **136**, B864 (1964)

[32] M. Levy, Proc. Natl. Acad. Sci. USA **76**, 6062 (1979)

[33] W. Kohn and L.J. Sham, Phys. Rev. **140**, A1133 (1965)

[34] U.V. Barth and L. Hedin, J. Phys. C: Solid State Phys. **5**, 1629 (1972)

[35] J.P. Perdew, K. Burke, and M. Ernzerhof, Phys. Rev. Lett. **77**, 3865 (1996)

[36] J. Heyd, G.E. Scuseria, and M. Ernzerhof, J. Chem. Phys. **118**, 8207 (2003)

[37] V.I. Anisimov, J. Zaanen, and O.K. Andersen, Phys. Rev. B **44**, 943 (1991)

[38] P. Pulay, J. Comp. Chem. **3** (1982)

[39] D. Vanderbilt and S.G. Louie, Phys. Rev. B **30**, 6118 (1984)

[40] L.D. Marks and D.R. Luke, Phys. Rev. B **78**, 075114 (2008)

[41] N.D. Woods, M.C. Payne, and P.J. Hasnip, J. Phys.: Condens. Matter **31**, 453001 (2019)

[42] X. Gonze, Phys. Rev. B **54**, 4383 (1996)

[43] O. Gunnarsson and B. Lundqvist, Phys. Rev. B **13**, 4274 (1976)

[44] W. Yang and P.W. Ayers, arXiv:2403.04604

[45] S. Kundu and D. Sénéchal, SciPost Phys. Core **7**, 033 (2024)

[46] P. Kurz, F. Förster, L. Nordström, G. Bihlmayer, and S. Blügel, Phys. Rev. B **69**, 024415 (2004)

[47] L.D. Landau and E.M. Lifshitz, Phys. Z. Sowjetunion **8**, 153 (1935)

[48] B. Huang, G. Clark, E. Navarro-Moratalla, D.R. Klein, R. Cheng, K.L. Seyler, D. Zhong, E. Schmidgall, M.A. McGuire, D.H. Cobden, W. Yao, D. Xiao, P. Jarillo-Herrero, and X. Xu, Nature **546**, 270 (2017)

[49] P. Delugas, O. Baseggio, I. Timrov, S. Baroni, and T. Gorni, Phys. Rev. B **107**, 214452 (2023)